

Quasilinear theory of the diocotron instability for nonrelativistic non-neutral electron flow in planar geometry

Ronald C. Davidson

Citation: [The Physics of Fluids](#) **28**, 1937 (1985); doi: 10.1063/1.864938

View online: <https://doi.org/10.1063/1.864938>

View Table of Contents: <https://aip.scitation.org/toc/pfl/28/6>

Published by the [American Institute of Physics](#)

ARTICLES YOU MAY BE INTERESTED IN

[Diocotron Instability in Plasmas and Gas Discharges](#)

[Journal of Applied Physics](#) **37**, 602 (1966); <https://doi.org/10.1063/1.1708223>

[Diocotron Instability in a Cylindrical Geometry](#)

[The Physics of Fluids](#) **8**, 1288 (1965); <https://doi.org/10.1063/1.1761400>

[Influence of profile shape on the diocotron instability in a non-neutral plasma column](#)

[Physics of Plasmas](#) **5**, 3497 (1998); <https://doi.org/10.1063/1.873067>

[Diocotron instability for intense relativistic non-neutral electron flow in planar diode geometry](#)

[The Physics of Fluids](#) **31**, 1727 (1988); <https://doi.org/10.1063/1.866711>

[Non-modal analysis of the diocotron instability: Plane geometry](#)

[Physics of Plasmas](#) **19**, 082112 (2012); <https://doi.org/10.1063/1.4747506>

[Coherent structures and turbulence evolution in magnetized non-neutral plasmas](#)

[AIP Conference Proceedings](#) **1928**, 020012 (2018); <https://doi.org/10.1063/1.5021577>

Quasilinear theory of the diocotron instability for nonrelativistic non-neutral electron flow in planar geometry

Ronald C. Davidson

Plasma Fusion Center, Massachusetts Institute of Technology, Cambridge, Massachusetts 02139

(Received 22 October 1984; accepted 3 February 1985)

A macroscopic cold-fluid model is used to investigate the quasilinear stabilization of the diocotron instability for sheared, nonrelativistic electron flow. Planar diode geometry is assumed, with cathode and anode located at $x = 0$ and $x = d$, respectively. The non-neutral plasma is immersed in a strong applied magnetic field $B_0 \hat{e}_z$, and the electrons are treated as a massless ($m \rightarrow 0$) guiding-center fluid with flow velocity $\mathbf{V}_b = -(c/B_0) \nabla \phi \times \hat{e}_z$, where $\partial/\partial z = 0$ is assumed, and the fields are electrostatic with $\mathbf{E} = -\nabla \phi$. All quantities are assumed to be periodic in the y direction with periodicity length L . The nonlinear continuity-Poisson equations are used to obtain coupled quasilinear kinetic equations describing the self-consistent evolution of the average density $\langle n_b \rangle(x, t)$ and spectral energy density $\mathcal{E}_k(x, t)$ associated with the y -electric field perturbations. Here, the average flow velocity in the y direction is $V_E(x, t) = (c/B_0)(\partial/\partial x)\langle \phi \rangle(x, t)$, where average quantities are defined by $\langle \psi \rangle(x, t) = \int_0^L (dy/L) \psi(x, y, t)$. Several general features of the quasilinear evolution of the system are discussed, including a derivation of exact conservation constraints. Typically, if the initial profile $\langle n_b \rangle(x, t = 0)$ corresponds to instability with $\gamma_k(0) > 0$, the perturbations amplify, and the density profile $\langle n_b \rangle(x, t)$ readjusts in such a way as to reduce the growth rate $\gamma_k(t)$ and stabilize the instability. As a specific example, the quasilinear evolution of the diocotron instability is considered for $\langle n_b \rangle(x, 0)$ corresponding to a gentle density bump superimposed on a rectangular density profile in contact with the cathode.

I. INTRODUCTION AND SUMMARY

One of the most ubiquitous instabilities in low-density ($\omega_{pb}^2 \ll \omega_c^2$) non-neutral plasmas with velocity shear is the classical diocotron instability.¹⁻⁸ For example, the diocotron instability can occur in propagating non-neutral electron beams and layers⁷⁻¹² and in low-voltage microwave generation devices such as magnetrons, traveling wave tubes, and ubitrons.^{13,14} While the linear theory of the diocotron instability has been extensively developed in the literature, there has been little work on the nonlinear response of the system to the amplifying field perturbations. As an attempt to delineate some of the fundamental physics issues associated with the nonlinear development of instabilities driven by velocity shear in non-neutral plasmas, we develop here a detailed quasilinear description of the classical diocotron instability.

The present analysis makes use of a macroscopic cold-fluid model to describe sheared, nonrelativistic electron flow in planar geometry (Fig. 1). The low-density non-neutral electron plasma is immersed in a strong applied magnetic field $B_0 \hat{e}_z$, and the electrons are treated as a massless ($m \rightarrow 0$), guiding-center fluid with flow velocity $\mathbf{V}_b = -c \nabla \phi \times \hat{e}_z / B_0$. The nonlinear continuity-Poisson equations are then used to obtain coupled quasilinear kinetic equations that describe the self-consistent evolution of the average density profile $\langle n_b \rangle(x, t)$ and the spectral energy density associated with the amplifying electric field perturbations. As illustrated in Fig. 1, the present analysis assumes planar diode geometry, with cathode and anode located at $x = 0$ and $x = d$, respectively. However, it should be emphasized that the quasilinear model of the diocotron instability developed in Secs. II-IV is quite general, and can be extended to other configurations with straightforward modifications. For example, the formalism is readily extended to the case where the con-

ducting walls are far removed from the plasma (or absent entirely).

It should also be pointed out that a closely related instability (often called the magnetron instability)¹⁵⁻¹⁷ occurs for sheared non-neutral electron flow at higher density, where space-charge effects are even stronger. This instability¹⁵⁻¹⁷ can play an important role in high-voltage diodes with application to the generation of intense charged particle beams for inertial confinement fusion.¹⁸ In this regard, for non-neutral electron flow in high-voltage diodes, the analysis in Secs. II-IV must be extended to include relativistic and electromagnetic effects as well as electron inertial effects.

The following is a brief outline of the paper. The analysis assumes that $\partial/\partial z = 0$ and the fields are electrostatic with $\mathbf{E}(x, y, t) = -\nabla \phi(x, y, t)$. The cold-fluid model described in Sec. II is based on the continuity-Poisson equations [Eqs. (7) and (8)], which describe the self-consistent nonlinear evolution of the electron density $n_b(x, y, t)$ and the electrostatic potential $\phi(x, y, t)$. Quantities are expressed as an average val-

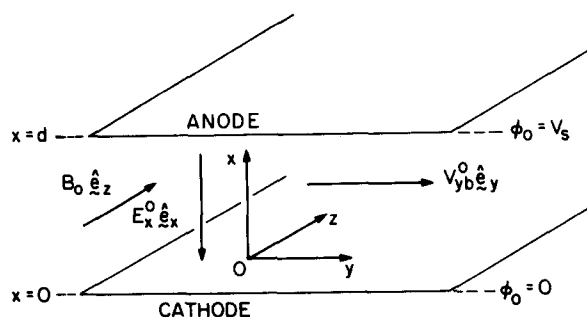


FIG. 1. Planar diode configuration with $\mathbf{B}_0 = B_0 \hat{e}_z$, and cathode and anode located at $x = 0$ and $x = d$, respectively.

ue (averaged over y) plus a perturbation, e.g., $n_b(x, y, t) = \langle n_b \rangle(x, t) + \delta n_b(x, y, t)$, where $\langle n_b \rangle \equiv \int_0^L (dy/L) n_b(x, y, t)$, $\langle \delta n_b \rangle = 0$, and L is the periodicity length in the y direction (Fig. 1). It is found, for example, that the average density profile $\langle n_b \rangle(x, t)$ evolves nonlinearly according to Eq. (14). Therefore, as the perturbations δn_b and $\delta \phi$ amplify, there is a corresponding readjustment of the density profile $\langle n_b \rangle(x, t)$ and flow velocity $V_E(x, t) = (c/B_0) (\partial/\partial x) \langle \phi \rangle(x, t)$ in response to the instability.

In Secs. III and IV, the formalism developed in Sec. II is used to obtain a lowest-order nonlinear (i.e., quasilinear) description of the evolution of the average density profile $\langle n_b \rangle(x, t)$ and the spectral energy density $\mathcal{E}_k(x, t) = (k^2 |\delta \phi_k(x)|^2 / 8\pi) \exp[2 \int_0^t dt' \gamma_k(t')]$ in the y electric field perturbations, $\delta E_y(x, y, t) = -(\partial/\partial y) \times \delta \phi(x, y, t)$. The quasilinear analysis assumes that the initial density profile $\langle n_b \rangle(x, 0)$ corresponds to linear instability with $\gamma_k(0) > 0$. Moreover, bilinear nonlinearities (proportional to $\delta n_b \delta \phi$) are neglected in describing the evolution of $\delta n_b(x, y, t)$. To briefly summarize, we obtain coupled kinetic equations for the average density profile $\langle n_b \rangle(x, t)$ and spectral energy density $\mathcal{E}_k(x, t)$ [Eqs. (55) and (57)], where the diffusion coefficient $D(x, t)$ is defined in Eq. (56), and the complex oscillation frequency $\omega_k + i\gamma_k$ is determined adiabatically in time from the eigenvalue equation (58). General features of the quasilinear evolution of the system are described in Sec. IV B, including exact conservation constraints. Typically, if the initial profile $\langle n_b \rangle(x, t=0)$ corresponds to instability with $\gamma_k(0) > 0$, the perturbations will amplify, and the density profile $\langle n_b \rangle(x, t)$ will readjust in such a way as to reduce the growth rate $\gamma_k(t)$ and stabilize the instability.

As a specific example, in Sec. IV C we consider the quasilinear evolution of the diocotron instability for $\langle n_b \rangle(x, 0)$ corresponding to a gentle density bump superimposed on a rectangular density profile in contact with the cathode. Such a configuration gives a weak resonant version of the diocotron instability with $|\gamma_k| \ll |\omega_k|$ and growth rate given by Eq. (81). It is shown that the system stabilizes time asymptotically by plateau formation with $(\partial/\partial x) \langle n_b \rangle(x, t \rightarrow \infty)|_{x=x_s} = 0$ and $\gamma_k(t \rightarrow \infty) = 0$ [Eq. (92)], where the resonant location x_s is determined from $\omega_k - kV_E(x_s) = 0$. Finally, for the configuration with gentle density bump considered in Sec. IV C, we also make use of the quasilinear equations to obtain an order-of-magnitude estimate of the saturation level of the perturbed fields.

II. THEORETICAL MODEL

In this section, we discuss various general aspects of the theoretical model and assumptions (Sec. II A), the nonlinear evolution of average quantities (Sec. II B), the nonlinear evolution of perturbed quantities (Sec. II C), and boundary conditions at the cathode and anode (Sec. II D).

A. Theoretical model and assumptions

We consider here the nonrelativistic flow of a cold, non-neutral pure electron plasma confined in the planar diode configuration illustrated in Fig. 1. The cathode is located at $x = 0$ and the anode at $x = d$. The electron fluid is immersed

in a uniform applied magnetic field $B_0 \hat{e}_z$. The analysis is based on a macroscopic cold-fluid description with the following simplifying assumptions.

(a) All fluid and field quantities are assumed to be independent of z ($\partial/\partial z = 0$) and spatially periodic in the y direction with periodicity length L . For example, the electron density $n_b(x, t)$ satisfies $n_b(x, y + L, t) = n_b(x, y, t)$.

(b) The fields are assumed to be electrostatic with electric field

$$\mathbf{E}(x, t) = -\nabla \phi(x, y, t), \quad (1)$$

and magnetic field $B_0 \hat{e}_z$.

(c) In the present analysis the electrons are treated as a cold, massless ($m \rightarrow 0$), guiding-center fluid with flow velocity $\mathbf{V}_b = c\mathbf{E} \times \hat{e}_z / B_0$, i.e.,^{2,4}

$$\mathbf{V}_b(x, t) = -(c/B_0) \nabla \phi \times \hat{e}_z. \quad (2)$$

Equivalently, Eq. (2) can be expressed as

$$V_{bx}(x, y, t) = -\frac{c}{B_0} \frac{\partial}{\partial y} \phi(x, y, t), \quad (3)$$

$$V_{by}(x, y, t) = \frac{c}{B_0} \frac{\partial}{\partial x} \phi(x, y, t).$$

A cold electron fluid model with $\mathbf{E} + \mathbf{V}_b \times B_0 \hat{e}_z / c = 0$ [Eq. (2)] is valid provided the electron density is sufficiently low and perturbations have sufficiently low frequency that^{2,4,5,19}

$$\omega_{pb}^2 \ll \omega_c^2, \quad \left| \frac{\partial}{\partial t} \right| \ll \omega_c. \quad (4)$$

Here $\omega_c = eB_0/mc$ is the electron-cyclotron frequency, $\omega_{pb}^2 = 4\pi n_b e^2/m$ is the electron plasma frequency-squared, and $-e$ and m are the electron charge and rest mass, respectively. Note from Eq. (2) that the electron flow in the present model is incompressible with $\nabla \cdot \mathbf{V}_b = 0$.

(d) Finally, it is also assumed that the equilibrium electron flow is space-charge limited. That is, under steady-state ($\partial/\partial t = 0$) conditions, the electrostatic potential $\phi_0(x)$ satisfies

$$E_x^0(x=0) = -\frac{\partial \phi_0}{\partial x} \Big|_{x=0} = 0, \quad (5)$$

$$\phi_0(x=0) = 0, \quad \phi_0(x=d) = V_s,$$

where the anode voltage V_s is related to the electron density profile $n_b^0(x)$ by¹⁵⁻¹⁷

$$V_s = 4\pi e \int_0^d dx'' \int_0^{x''} dx' n_b^0(x'). \quad (6)$$

Equation (6) follows from solving $\partial^2 \phi_0 / \partial x^2 = 4\pi e n_b^0(x)$ in the anode-cathode gap and enforcing the boundary conditions in Eq. (5).

Within the context of assumptions (a)-(c), the electron density $n_b(x, y, t)$ and electrostatic potential $\phi(x, y, t)$ are determined self-consistently from Poisson's equation and the equation of continuity, i.e.,

$$\left(\frac{\partial^2}{\partial x^2} + \frac{\partial^2}{\partial y^2} \right) \phi = 4\pi e n_b, \quad (7)$$

and

$$\frac{\partial n_b}{\partial t} + \frac{\partial}{\partial x} (n_b V_{bx}) + \frac{\partial}{\partial y} (n_b V_{by}) = 0. \quad (8)$$

Making use of Eq. (3) to eliminate V_{bx} and V_{by} in favor of ϕ , the continuity equation (8) can be expressed in the equivalent form

$$\frac{\partial n_b}{\partial t} - \frac{c}{B_0} \left[\frac{\partial}{\partial x} \left(n_b \frac{\partial \phi}{\partial y} \right) - \frac{\partial}{\partial y} \left(n_b \frac{\partial \phi}{\partial x} \right) \right] = 0. \quad (9)$$

Equations (7) and (9) constitute coupled equations describing the nonlinear evolution of the electrostatic potential $\phi(x, y, t)$ and the electron density $n_b(x, y, t)$.

B. Nonlinear evolution of average quantities

In the analysis that follows, it is convenient to express all field and fluid quantities as an average value (averaged over y) plus a perturbation. That is, a general quantity $\psi(x, y, t)$ is expressed as

$$\psi(x, y, t) = \langle \psi \rangle(x, t) + \delta \psi(x, y, t), \quad (10)$$

where the average value $\langle \psi \rangle(x, t)$ is defined by

$$\langle \psi \rangle(x, t) \equiv \frac{1}{L} \int_0^L dy \psi(x, y, t). \quad (11)$$

Here, L is the periodicity length in the y direction, and it follows from Eqs. (10) and (11) that $\langle \delta \psi \rangle = 0$.

Averaging Poisson's equation (7) over y , we find that

$$\frac{\partial^2}{\partial x^2} \langle \phi \rangle = 4\pi e \langle n_b \rangle, \quad (12)$$

which relates the average potential $\langle \phi \rangle(x, t)$ to the average density $\langle n_b \rangle(x, t)$. Moreover, averaging the continuity equation (9) over y and making use of periodicity in the y direction gives

$$\frac{\partial}{\partial t} \langle n_b \rangle = \frac{c}{B_0} \frac{\partial}{\partial x} \left\langle n_b \frac{\partial \phi}{\partial y} \right\rangle \quad (13)$$

for the evolution of $\langle n_b \rangle$. Expressing $n_b(x, y, t) = \langle n_b \rangle(x, t) + \delta n_b(x, y, t)$ and $\phi(x, y, t) = \langle \phi \rangle(x, t) + \delta \phi(x, y, t)$ on the right-hand side of Eq. (13), and making use of $(\partial/\partial y)\langle \phi \rangle = 0$ and $\langle \delta n_b \rangle = 0$, it readily follows that Eq. (13) can be expressed in the equivalent form

$$\frac{\partial}{\partial t} \langle n_b \rangle = \frac{c}{B_0} \frac{\partial}{\partial x} \left\langle \delta n_b \frac{\partial \phi}{\partial y} \right\rangle, \quad (14)$$

which describes the (slow) nonlinear evolution of the average density profile $\langle n_b \rangle(x, t)$ in response to the perturbations δn_b and $\delta \phi$.

C. Nonlinear evolution of perturbed quantities

In Eqs. (7) and (9), we express the potential $\phi(x, y, t)$ and electron density $n_b(x, y, t)$ as average values plus perturbations, i.e.,

$$\phi(x, y, t) = \langle \phi \rangle(x, t) + \delta \phi(x, y, t), \quad (15)$$

$$n_b(x, y, t) = \langle n_b \rangle(x, t) + \delta n_b(x, y, t),$$

where $\langle \phi \rangle$ and $\langle n_b \rangle$ evolve according to Eqs. (12) and (14). Subtracting Eq. (12) from Eq. (7) gives Poisson's equation for the perturbed potential $\delta \phi(x, y, t)$,

$$\left(\frac{\partial^2}{\partial x^2} + \frac{\partial^2}{\partial y^2} \right) \delta \phi = 4\pi e \delta n_b. \quad (16)$$

On the other hand, substituting Eq. (15) into the continuity equation (9) and making use of $(\partial/\partial y)\langle \phi \rangle = 0$, we find

$$\begin{aligned} \frac{\partial}{\partial t} (\langle n_b \rangle + \delta n_b) - \frac{c}{B_0} \frac{\partial}{\partial x} \left((\langle n_b \rangle + \delta n_b) \frac{\partial \delta \phi}{\partial y} \right) \\ + \frac{c}{B_0} \frac{\partial}{\partial y} \left((\langle n_b \rangle + \delta n_b) \frac{\partial}{\partial x} (\langle \phi \rangle + \delta \phi) \right) = 0. \end{aligned} \quad (17)$$

Defining the average $\mathbf{E} \times \mathbf{B}_0 \hat{e}_z$ flow velocity in the y direction by

$$V_E(x, t) = -\frac{c \langle E_x \rangle}{B_0} = \frac{c}{B_0} \frac{\partial}{\partial x} \langle \phi \rangle(x, t), \quad (18)$$

and eliminating $\partial \langle n_b \rangle / \partial t$ from Eq. (17) by means of Eq. (14), it follows that Eq. (17) can be expressed in the equivalent form

$$\begin{aligned} \left(\frac{\partial}{\partial t} + V_E \frac{\partial}{\partial y} \right) \delta n_b - \frac{c}{B_0} \left(\frac{\partial}{\partial y} \delta \phi \right) \frac{\partial}{\partial x} \langle n_b \rangle \\ = \frac{c}{B_0} \left[\left(\frac{\partial}{\partial y} \delta \phi \right) \left(\frac{\partial}{\partial x} \delta n_b \right) - \left(\frac{\partial}{\partial x} \delta \phi \right) \left(\frac{\partial}{\partial y} \delta n_b \right) \right. \\ \left. - \frac{\partial}{\partial x} \langle \delta n_b \frac{\partial \delta \phi}{\partial y} \rangle \right]. \end{aligned} \quad (19)$$

In Eq. (19), we have transposed all terms explicitly bilinear in $\delta \phi \delta n_b$ to the right-hand side.

Equations (12) and (16) for $\langle \phi \rangle(x, t)$ and $\delta \phi(x, y, t)$, and Eqs. (14) and (19) for $\langle n_b \rangle(x, t)$ and $\delta n_b(x, y, t)$ constitute a closed description of the nonlinear evolution of the system, which is fully equivalent to the Poisson-continuity equations (7) and (9). In circumstances where the initial density profile $\langle n_b \rangle(x, 0)$ corresponds to linear instability, the perturbations $\delta \phi$ and δn_b amplify, and the average density profile $\langle n_b \rangle(x, t)$ readjusts in response to the unstable field perturbations according to Eq. (14).

A lowest-order *quasilinear* analysis (Sec. III)²⁰ of Eqs. (12), (14), (16), and (19) proceeds by neglecting all bilinear nonlinearities on the right-hand side of Eq. (19) for δn_b . The resulting equation for δn_b is then solved in conjunction with Eq. (16) for $\delta \phi$, and the resulting expressions are substituted into Eq. (14) to determine the quasilinear response of the average density profile $\langle n_b \rangle(x, t)$ to the unstable field perturbations.

D. Boundary conditions

For completeness, we conclude this section with a brief discussion of the boundary conditions assumed in the present analysis. In particular, it is assumed that there is zero net flux of electrons at the cathode ($x = 0$) and at the anode ($x = d$), i.e., $n_b V_{xb} = 0$ at $x = 0$ and $x = d$. Equivalently, from Eq. (3), this condition can be expressed as

$$E_y = -\frac{\partial}{\partial y} \phi = 0, \quad \text{at } x = 0 \text{ and } x = d, \quad (20)$$

or $(\partial/\partial y)\delta \phi = 0$ at $x = 0$ and $x = d$, since $(\partial/\partial y)\langle \phi \rangle = 0$. It then follows directly from Eqs. (20) and (14) [or Eq. (13)] that

$$\frac{\partial}{\partial t} \int_0^d dx \langle n_b \rangle = 0. \quad (21)$$

That is, however complicated the nonlinear evolution of the average density profile $\langle n_b \rangle(x, t)$, the total number of electrons in the cathode-anode region is conserved. Of course, this is expected because of the zero-net-flux boundary conditions at the cathode and anode [Eq. (20)].

Finally, assuming that space-charge limited flow is maintained with $\langle E_x \rangle = -(\partial/\partial x)\langle \phi \rangle = 0$ at $x = 0$, it follows from Poisson's equation (12) for $\langle \phi \rangle$ that $\langle \phi \rangle$ and $\langle n_b \rangle$ are related by

$$\langle \phi \rangle(x, t) = 4\pi e \int_0^x dx'' \int_0^{x''} dx' \langle n_b \rangle(x', t), \quad (22)$$

where $\langle \phi \rangle = 0$ at $x = 0$. Evaluating Eq. (22) at $x = d$, we find that the anode voltage $V_s(t)$ consistent with space-charge-limited flow is given by

$$V_s(t) = 4\pi e \int_0^d dx'' \int_0^{x''} dx' \langle n_b \rangle(x', t). \quad (23)$$

III. QUASILINEAR THEORY OF DIOCOTRON INSTABILITY

A. Quasilinear kinetic equations

With regard to Poisson's equation (16) for $\delta\phi$ and the continuity equation (19) for δn_b , it is convenient to Fourier decompose perturbed quantities with respect to their y dependence. That is, we express

$$\delta\phi(x, y, t) = \sum_k \delta\phi_k(x, t) \exp(iky), \quad (24)$$

$$\delta n_b(x, y, t) = \sum_k \delta n_{bk}(x, t) \exp(iky),$$

where $k = 2\pi n/L$, L is the periodicity length in the y direction, n is an integer, and the summation is from $n = -\infty$ to $n = +\infty$. Equation (16) then gives

$$\frac{\partial^2}{\partial x^2} \delta\phi_k - k^2 \delta\phi_k = 4\pi e \delta n_{bk}, \quad (25)$$

which relates $\delta\phi_k(x, t)$ and $\delta n_{bk}(x, t)$. At the quasilinear level of description (see discussion at the end of Sec. II C), the right-hand side of Eq. (19) is approximated by zero, corresponding to the neglect of bilinear nonlinearities in the evolution of δn_b . Fourier decomposing Eq. (19) then gives

$$\left(\frac{\partial}{\partial t} + ikV_E \right) \delta n_{bk} = \frac{ikc}{B_0} \delta\phi_k \frac{\partial}{\partial x} \langle n_b \rangle, \quad (26)$$

where [from Eqs. (18) and (22)] $V_E(x, t)$ is given by

$$V_E(x, t) = \frac{c}{B_0} \frac{\partial}{\partial x} \langle \phi \rangle = \frac{4\pi ec}{B_0} \int_0^x dx' \langle n_b \rangle(x', t). \quad (27)$$

In Eqs. (26) and (27), the (slow) evolution of $\langle n_b \rangle(x, t)$ is calculated self-consistently in terms of $\delta\phi$ and δn_b from Eq. (14), which can be expressed in Fourier variables as

$$\frac{\partial}{\partial t} \langle n_b \rangle = \frac{c}{B_0} \frac{\partial}{\partial x} \sum_k \delta n_{bk} (-ik) \delta\phi_{-k}. \quad (28)$$

Equations (25)–(28) constitute coupled nonlinear equations for the evolution of $\delta\phi_k$, δn_{bk} , and $\langle n_b \rangle$ at the quasilinear level of description.

To analyze Eqs. (25) and (26), we consider amplifying ($\gamma_k > 0$) perturbations with time dependence of the form

$$\delta\phi_k(x, t) = \delta\hat{\phi}_k(x) \exp\left(\int_0^t dt' [-i\omega_k(t') + \gamma_k(t')]\right), \quad (29)$$

$$\delta n_{bk}(x, t) = \delta\hat{n}_{bk}(x) \exp\left(\int_0^t dt' [-i\omega_k(t') + \gamma_k(t')]\right).$$

In Eq. (29), the growth rate $\gamma_k(t)$ and oscillation frequency $\omega_k(t)$ are allowed to vary slowly in time in response to the slow evolution of $\langle n_b \rangle(x, t)$ in Eq. (28). Substituting Eq. (29) into Eq. (26) and solving for δn_{bk} gives

$$\delta n_{bk} = \frac{-(kc/B_0)\delta\phi_k}{\omega_k - kV_E + i\gamma_k} \frac{\partial}{\partial x} \langle n_b \rangle. \quad (30)$$

Moreover, substituting Eq. (30) into Eq. (25), Poisson's equation for $\delta\phi_k$ becomes

$$\frac{\partial^2}{\partial x^2} \delta\phi_k - k^2 \delta\phi_k = \frac{-(4\pi e kc/B_0)\delta\phi_k}{\omega_k - kV_E + i\gamma_k} \frac{\partial}{\partial x} \langle n_b \rangle, \quad (31)$$

where $\gamma_k > 0$ is assumed. Note that Eqs. (30) and (31) are identical in form to the equations for δn_{bk} and $\delta\phi_k$ obtained in standard linear theory,^{2,4,5} assuming perturbations about quasisteady equilibrium profiles $\langle n_b \rangle$ and V_E . The only difference in the present *quasilinear* analysis is that $\langle n_b \rangle(x, t)$ is allowed to vary slowly in time [Eq. (28)], which leads to a corresponding slow (adiabatic) variation in the growth rate $\gamma_k(t)$ and oscillation frequency $\omega_k(t)$ as calculated from the eigenvalue equation (31).²⁰

Substituting Eq. (30) into Eq. (28), the average density profile $\langle n_b \rangle(x, t)$ evolves according to

$$\frac{\partial}{\partial t} \langle n_b \rangle = \left(\frac{c}{B_0} \right)^2 \frac{\partial}{\partial x} \left(\sum_k \frac{ik^2 |\delta\phi_k|^2}{\omega_k - kV_E + i\gamma_k} \frac{\partial}{\partial x} \langle n_b \rangle \right). \quad (32)$$

In obtaining Eq. (32), use has been made of the conjugate symmetry

$$\delta\phi_{-k}(x, t) = \delta\phi_k^*(x, t), \quad (33)$$

which follows from Eq. (24) since $\delta\phi(x, y, t)$ is a real-valued function. Consistent with Eq. (33), it follows from Eq. (29) that the oscillation frequency ω_k and growth rate γ_k satisfy the symmetries

$$\omega_{-k} = -\omega_k, \quad \gamma_{-k} = \gamma_k, \quad (34)$$

and the amplitude $\delta\hat{\phi}_k(x)$ satisfies $\delta\hat{\phi}_{-k} = \delta\hat{\phi}_k^*$. Making use of

$$\frac{1}{\omega_k - kV_E + i\gamma_k} = \frac{(\omega_k - kV_E) - i\gamma_k}{(\omega_k - kV_E)^2 + \gamma_k^2}$$

and the symmetries in Eq. (34) to eliminate the odd functions of k on the right-hand side of Eq. (32), we find that the quasilinear kinetic equation for $\langle n_b \rangle$ can be expressed as

$$\frac{\partial}{\partial t} \langle n_b \rangle = \frac{\partial}{\partial x} \left(D(x, t) \frac{\partial}{\partial x} \langle n_b \rangle \right), \quad (35)$$

where the diffusion coefficient $D(x, t)$ is defined by

$$D(x, t) = \left(\frac{c}{B_0} \right)^2 \sum_k \frac{k^2 |\delta\phi_k|^2 \gamma_k}{(\omega_k - kV_E)^2 + \gamma_k^2}, \quad (36)$$

and $\gamma_k > 0$ is assumed. Moreover, from Eq. (29), the quantity $|\delta\phi_k|^2$ evolves according to

$$\frac{\partial}{\partial t} |\delta\phi_k|^2 = 2\gamma_k |\delta\phi_k|^2. \quad (37)$$

To summarize, the quasilinear evolution of $\langle n_b \rangle$ and $|\delta\phi_k|^2$ is described by the coupled kinetic equations (35) and (37), where the diffusion coefficient D is defined in Eq. (36). Moreover, the growth rate $\gamma_k(t)$ and oscillation frequency $\omega_k(t)$ are determined adiabatically from the linear eigenvalue equation (31) with $\langle n_b \rangle$ changing slowly in time according to the kinetic equation (35). Typically, if the initial profile $\langle n_b \rangle(x, t=0)$ corresponds to instability with $\gamma_k(0) > 0$, the perturbations will amplify [Eq. (37)], and the density profile $\langle n_b \rangle(x, t)$ will readjust [Eq. (35)] in such a way as to reduce the growth rate $\gamma_k(t)$ and stabilize the instability [Eqs. (31) and (37)].

For future reference, we consider Eqs. (36) and (37) in the limit of a continuous k spectrum with

$$\sum_k \frac{k^2 |\delta\phi_k|^2}{8\pi} \dots \rightarrow \int dk \mathcal{E}_k \dots \quad (38)$$

Here, $\mathcal{E}_k = k^2 |\delta\phi_k|^2 / 8\pi$ is the spectral energy density associated with the δE_y electric field perturbations. In the continuum limit, Eqs. (36) and (37) become

$$D(x, t) = \frac{8\pi c^2}{B_0^2} \int dk \frac{\gamma_k \mathcal{E}_k}{(\omega_k - kV_E)^2 + \gamma_k^2}, \quad (39)$$

and

$$\frac{\partial}{\partial t} \mathcal{E}_k = 2\gamma_k \mathcal{E}_k, \quad (40)$$

where γ_k is the linear growth rate determined from Eq. (31).

B. Quasilinear growth rate

The growth rate γ_k and oscillation frequency ω_k are determined from the eigenvalue equation (31). In terms of the amplitude $\delta\hat{\phi}_k(x)$ [Eq. (29)], Eq. (31) can be expressed as

$$\frac{\partial^2}{\partial x^2} \delta\hat{\phi}_k - k^2 \delta\hat{\phi}_k = - \frac{k \delta\hat{\phi}_k}{\omega_k - kV_E + i\gamma_k} \frac{4\pi e^2}{m\omega_c} \frac{\partial}{\partial x} \langle n_b \rangle, \quad (41)$$

where $\omega_c = eB_0/mc$ is the electron-cyclotron frequency. For specified $\langle n_b \rangle$ and corresponding self-consistent flow velocity V_E [Eq. (27)], Eq. (41) can be solved for the eigenfunction $\delta\hat{\phi}_k$ and complex eigenfrequency $\omega_k + i\gamma_k$. This has been done in the literature for a variety of unstable profiles.^{2,4,5}

Equation (41) can also be used to derive an effective dispersion relation for $\omega_k + i\gamma_k$ in circumstances where the functional form of $\delta\hat{\phi}_k(x)$ is known. Multiplying Eq. (41) by $\delta\hat{\phi}_k^* = \delta\hat{\phi}_k^*$ integrating from $x = 0$ to $x = d$, and making use of $\delta\hat{\phi}_k(x=0) = 0 = \delta\hat{\phi}_k(x=d)$ [Eq. (20)] give

$$0 = \epsilon(k, \omega_k + i\gamma_k) = \int_0^d dx \left(\left| \frac{\partial}{\partial x} \delta\hat{\phi}_k \right|^2 + k^2 |\delta\hat{\phi}_k|^2 - \frac{k |\delta\hat{\phi}_k|^2}{\omega_k - kV_E + i\gamma_k} \frac{4\pi e^2}{m\omega_c} \frac{\partial}{\partial x} \langle n_b \rangle \right). \quad (42)$$

For specified $\delta\hat{\phi}_k(x)$, Eq. (42) plays the role of a dispersion

relation that determines $\omega_k + i\gamma_k$. Setting real and imaginary parts of Eq. (42) separately equal to zero gives

$$0 = \text{Re } \epsilon = \epsilon_r = \int_0^d dx \left(\left| \frac{\partial}{\partial x} \delta\hat{\phi}_k \right|^2 + k^2 |\delta\hat{\phi}_k|^2 - \frac{k (\omega_k - kV_E) |\delta\hat{\phi}_k|^2}{(\omega_k - kV_E)^2 + \gamma_k^2} \frac{4\pi e^2}{m\omega_c} \frac{\partial}{\partial x} \langle n_b \rangle \right), \quad (43)$$

and

$$0 = \text{Im } \epsilon = \epsilon_i = k\gamma_k \frac{4\pi e^2}{m\omega_c} \int_0^d dx \frac{|\delta\hat{\phi}_k|^2}{(\omega_k - kV_E)^2 + \gamma_k^2} \frac{\partial}{\partial x} \langle n_b \rangle. \quad (44)$$

Equation (44) can be used to prove the well-known *sufficient condition for stability*. That is, if^{4,5}

$$\frac{\partial}{\partial x} \langle n_b \rangle \leq 0 \quad (45)$$

over the interval $0 < x < d$, then Eq. (41) does not support unstable solutions with $\gamma_k > 0$. That is, $\gamma_k \leq 0$ and the perturbations are damped or purely oscillatory for monotonic decreasing density profiles of the form illustrated in Fig. 2(a). Equivalently, a *necessary condition for instability* ($\gamma_k > 0$) is that $(\partial/\partial x) \langle n_b \rangle$ or $(\partial^2/\partial x^2) V_E$ [Eqs. (12) and (18)] change sign on the interval $0 < x < d$. Therefore, density profiles that are instantaneously of the form illustrated in Figs. 2(b)–2(d) are expected to yield the diocotron instability driven by a shear in the velocity profile V_E . Hollow density profiles [Figs. 2(b) and 2(c)] tend to give strong instability, whereas profiles with a gentle density bump [Fig. 2(d)] give a weak resonant instability characterized by relatively small growth rate γ_k .^{4,5}

For the case of weak resonant diocotron instability [Fig. 2(d)] characterized by $|\gamma_k| \ll |\omega_k|$, the effective dispersion relation (42) can be further simplified. For small γ_k , we approximate

$$0 = \epsilon(k, \omega_k + i\gamma_k) = \epsilon_r(k, \omega_k) + i \left(\epsilon_i(k, \omega_k) + \gamma_k \frac{\partial \epsilon_r}{\partial \omega_k} \right) + \dots, \quad (46)$$

and

$$\lim_{\gamma_k \rightarrow 0^+} \frac{1}{\omega_k - kV_E + i\gamma_k} = \frac{P}{\omega_k - kV_E} - i\pi \delta(\omega_k - kV_E), \quad (47)$$

where P denotes Cauchy principal value. Substituting Eqs. (42) and (47) into Eq. (46) gives

$$0 = \epsilon_r(k, \omega_k) = \int_0^d dx \left(\left| \frac{\partial}{\partial x} \delta\hat{\phi}_k \right|^2 + k^2 |\delta\hat{\phi}_k|^2 - \frac{kP |\delta\hat{\phi}_k|^2}{\omega_k - kV_E} \frac{4\pi e^2}{m\omega_c} \frac{\partial}{\partial x} \langle n_b \rangle \right), \quad (48)$$

and

$$\gamma_k = - \frac{\epsilon_i}{\partial \epsilon_r / \partial \omega_k} = - \pi \int_0^d dx |\delta\hat{\phi}_k|^2 \delta(\omega_k - kV_E) \frac{\partial}{\partial x} \langle n_b \rangle \times \left(\int_0^d dx \frac{|\delta\hat{\phi}_k|^2 P}{(\omega_k - kV_E)^2} \frac{\partial}{\partial x} \langle n_b \rangle \right)^{-1}. \quad (49)$$

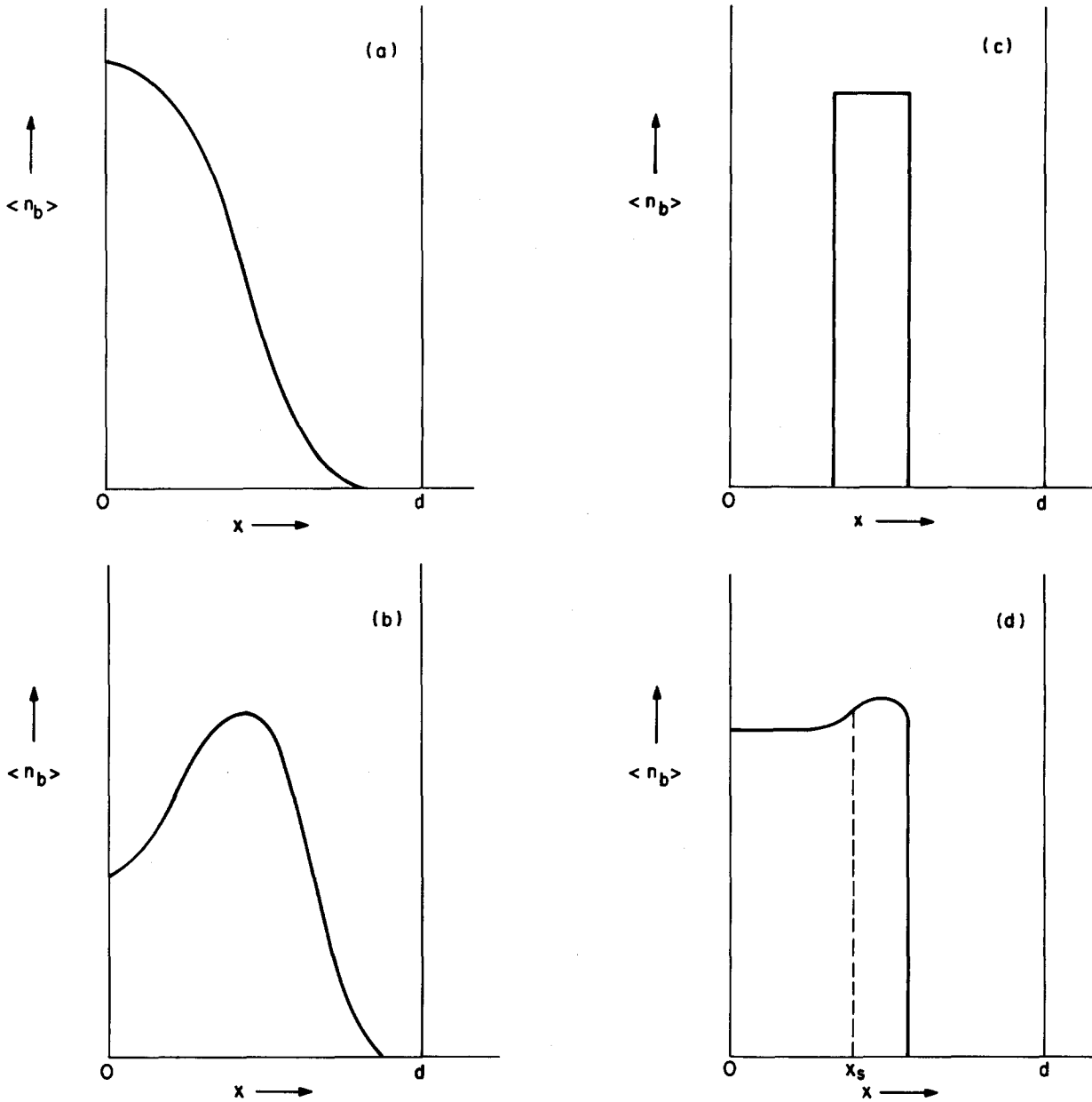


FIG. 2. Plot of $\langle n_b \rangle$ vs x for several density profiles with different stability properties. Solutions to eigenvalue equation (41) correspond to: (a) stable oscillations; (b) and (c) strong diocotron instability; and (d) weak resonant diocotron instability.

Denoting by $x = x_s(k)$ the resonant layer where

$$\omega_k - kV_E(x_s) = 0, \quad (50)$$

it follows from Eq. (49) that the growth rate γ_k can be expressed as^{4,5}

$$\gamma_k = \pi \left(\frac{|\delta\hat{\phi}_k|^2}{|k \partial V_E / \partial x|} \frac{\partial}{\partial x} \langle n_b \rangle \right)_{x=x_s} \times \left(- \int_0^d dx \frac{|\delta\hat{\phi}_k|^2 P}{(\omega_k - kV_E)^2} \frac{\partial}{\partial x} \langle n_b \rangle \right)^{-1}. \quad (51)$$

For $\partial \epsilon_r / \partial \omega_k < 0$, and therefore $(\dots)^{-1} > 0$ in Eq. (51), it follows from the above expression that $\gamma_k > 0$ (corresponding to instability) whenever the resonant layer x_s falls in the region of positive density slope, i.e.,

$$\frac{\partial}{\partial x} \langle n_b \rangle \Big|_{x=x_s} > 0, \quad (52)$$

as illustrated in Fig. 2(d). In circumstances where the nonlinear response of the system described by Eqs. (35) and (37) is such that the density profile flattens in the vicinity of $x = x_s$ with $(\partial / \partial x) \langle n_b \rangle|_{x=x_s} \rightarrow 0$, it follows from Eq. (51) that $\gamma_k \rightarrow 0$ corresponding to marginal stability and saturation of the wave spectrum [Eq. (40)]. The quasilinear stabilization of the resonant diocotron instability driven by a gentle density bump is discussed in Sec. IV C.

For future reference and use in Sec. IV C, here we summarize the limiting forms of the diffusion coefficient D [Eq. (39)] for the case of weak resonant diocotron instability. In particular, taking $\gamma_k \rightarrow 0_+$ in Eq. (39) in the resonant region of x space where $\omega_k - kV_E = 0$, it follows that D can be approximated by

$$D_r(x, t) = \frac{8\pi^2 c^2}{B_0^2} \int dk \mathcal{E}_k \delta(\omega_k - kV_E). \quad (53)$$

On the other hand, in the nonresonant region of x space where $(\omega_k - kV_E)^2 \gg \gamma_k^2$, it follows from Eq. (39) that D can be approximated by

$$D_{nr}(x, t) = \frac{8\pi c^2}{B_0^2} \int dk \frac{\gamma_k \mathcal{E}_k}{(\omega_k - kV_E)^2}. \quad (54)$$

The approximate forms of D_r and D_{nr} in Eqs. (53) and (54) are calculated to the same accuracy as Eqs. (48) and (51) for ω_k and γ_k .

IV. STABILIZATION PROCESS

In this section, we make use of the formalism developed in Sec. III to describe several features of the quasilinear stabilization process, both in the general case (Sec. IV B) and in circumstances corresponding to weak resonant diocotron instability (Sec. IV C).

A. Summary of quasilinear equations

For convenient reference, here we summarize in one location the full set of equations used in the quasilinear description of the diocotron instability derived in Sec. III. In particular, the kinetic equation describing the evolution of the average density profile $\langle n_b \rangle(x, t)$ is given by [Eq. (35)]

$$\frac{\partial}{\partial t} \langle n_b \rangle = \frac{\partial}{\partial x} \left(D \frac{\partial}{\partial x} \langle n_b \rangle \right), \quad (55)$$

where the diffusion coefficient $D(x, t)$ is defined by [Eq. (39)]

$$D(x, t) = \frac{8\pi c^2}{B_0^2} \int dk \frac{\gamma_k \mathcal{E}_k}{(\omega_k - kV_E)^2 + \gamma_k^2} \quad (56)$$

for $\gamma_k > 0$, and the spectral energy density \mathcal{E}_k evolves according to [Eq. (40)]

$$\frac{\partial}{\partial t} \mathcal{E}_k = 2\gamma_k \mathcal{E}_k. \quad (57)$$

In Eqs. (55)–(57), the spectral energy density is defined by

$$\mathcal{E}_k = k^2 |\delta\phi_k|^2 / 8\pi = (k^2 |\delta\hat{\phi}_k(x)|^2 / 8\pi) \times \exp\left(2 \int_0^t dt' \gamma_k(t')\right),$$

where the eigenfunction $\delta\hat{\phi}_k(x)$ and the complex oscillation frequency $\omega_k + i\gamma_k$ are determined from the eigenvalue equation [Eq. (41)]

$$\frac{\partial^2}{\partial x^2} \delta\hat{\phi}_k - k^2 \delta\hat{\phi}_k = - \frac{k \delta\hat{\phi}_k}{\omega_k - kV_E + i\gamma_k} \frac{4\pi e^2}{m\omega_c} \frac{\partial}{\partial x} \langle n_b \rangle. \quad (58)$$

Moreover, the average flow velocity $V_E(x, t) = (c/B_0)(\partial/\partial x)\langle\phi\rangle$ in Eqs. (56) and (58) is defined by [Eq. (27)]

$$V_E = \frac{4\pi ec}{B_0} \int_0^x dx' \langle n_b \rangle(x', t), \quad (59)$$

where $\langle n_b \rangle$ evolves according to Eq. (55). Note from Eq. (58) that $\omega_k + i\gamma_k$ varies adiabatically in time in response to the slow evolution of $\langle n_b \rangle$ and V_E . Making use of Eq. (20), the eigenvalue equation (58) is to be solved subject to the boundary conditions

$$\delta\hat{\phi}_k = 0, \quad \text{at } x = 0 \text{ and } x = d. \quad (60)$$

Correspondingly, the spectral energy density satisfies $\mathcal{E}_k = 0$ at the cathode ($x = 0$) and at the anode ($x = d$), and it follows from Eq. (56) that

$$D = 0, \quad \text{at } x = 0 \text{ and } x = d. \quad (61)$$

In the limiting case of weak resonant diocotron instability driven by a gentle density bump [Fig. 2(d)], or in circumstances where a more general initial profile for $\langle n_b \rangle$ [Fig. 2(b), say] evolves according to Eqs. (55)–(59) to a regime characterized by weak resonant instability, it follows from the analysis in Sec. III B that $\langle n_b \rangle$ and \mathcal{E}_k evolve according to Eqs. (55) and (57). Here the diffusion coefficient D is approximated by [Eqs. (53) and (54)]

$$D \simeq \begin{cases} D_r = \frac{8\pi^2 c^2}{B_0^2} \int dk \mathcal{E}_k \delta(\omega_k - kV_E), \\ \quad \text{for } \omega_k - kV_E = 0, \\ D_{nr} = \frac{8\pi c^2}{B_0^2} \int dk \frac{\gamma_k \mathcal{E}_k}{(\omega_k - kV_E)^2}, \\ \quad \text{for } (\omega_k - kV_E)^2 \gg \gamma_k^2. \end{cases} \quad (62)$$

Explicit expressions for the eigenfunction $\delta\hat{\phi}_k$, the growth rate γ_k , and the oscillation frequency ω_k appearing in Eq. (62) must generally be determined from the eigenvalue equation (58). However, for specified $\delta\hat{\phi}_k$, it also follows from the analysis in Sec. III B that ω_k and γ_k can be estimated from Eqs. (48) and (51), respectively, for weak resonant instability.

B. General features of the stabilization process

Consider the smooth initial density profile $\langle n_b \rangle(x, t = 0)$ corresponding to instability illustrated by the solid curve in Fig. 3(a). Assume $\gamma_k(t = 0) > 0$ and nonzero initial excitation of $|\delta\phi_k|^2$. In Fig. 3(a), the density maximum at $t = 0$ is located at $x = x_m$. Moreover, from Eq. (59) and Fig. 3(a), the corresponding initial flow velocity profile $V_E(x, t = 0)$ has the form illustrated by the solid curve in Fig. 3(b), with inflection point [$V_E''(x, t = 0) = 0$] located at $x = x_m$.

Several important features of the general quasilinear development of the system follow directly from Eqs. (55)–(61).

(a) *Number conservation*: First, number conservation readily follows upon integrating Eq. (55) from $x = 0$ to $x = d$ and enforcing Eq. (61), i.e.,

$$\frac{\partial}{\partial t} \int_0^d dx \langle n_b \rangle(x, t) = 0. \quad (63)$$

[See also Eq. (21).]

(b) *Conservation of average x location*: Second, the density-weighted, average x location of the electrons is also conserved, i.e.,

$$\frac{\partial}{\partial t} \int_0^d dx x \langle n_b \rangle(x, t) = 0. \quad (64)$$

The proof of Eq. (64) proceeds as follows. Multiplying Eq. (55) by x , integrating from $x = 0$ to $x = d$, and enforcing Eq. (61) gives

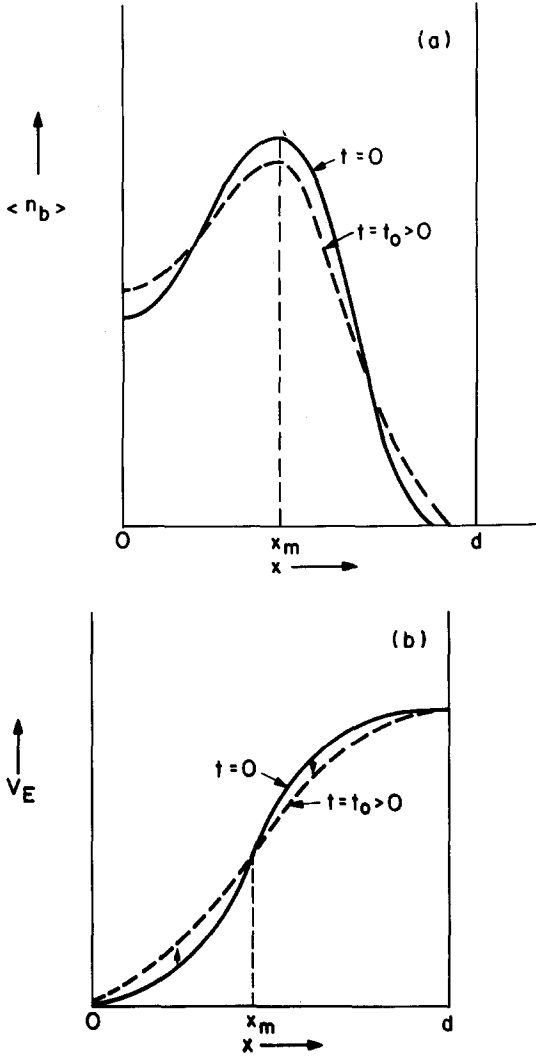


FIG. 3. Quasilinear response of (a) average density profile $\langle n_b \rangle(x, t)$ and (b) average flow velocity $V_E(x, t)$, in response to the amplifying field perturbations [Eqs. (55)–(59) and Eqs. (69)–(72)].

$$\frac{\partial}{\partial t} \int_0^d dx x \langle n_b \rangle = - \int_0^d dx D \frac{\partial}{\partial x} \langle n_b \rangle. \quad (65)$$

Multiplying the eigenvalue equation (31) by $(c/4\pi e B_0) k \delta \phi_{-k}$, integrating from $x=0$ to $x=d$, and integrating over k , we obtain

$$\begin{aligned} - \int_0^d dx \left(\frac{c}{B_0} \right)^2 \int dk \frac{k^2 |\delta \phi_k|^2}{\omega_k - k V_E + i \gamma_k} \frac{\partial}{\partial x} \langle n_b \rangle \\ = - \left(\frac{c}{4\pi e B_0} \right) \int_0^d dx \int dk k \left(\left| \frac{\partial}{\partial x} \delta \phi_k \right|^2 + k^2 |\delta \phi_k|^2 \right). \end{aligned} \quad (66)$$

The right-hand side of Eq. (66) vanishes identically since the integrand is an odd function of k . Equation (66) readily gives

$$\begin{aligned} - \int_0^d dx \left(\frac{c}{B_0} \right)^2 \int dk \frac{k^2 |\delta \phi_k|^2}{\omega_k - k V_E + i \gamma_k} \frac{\partial}{\partial x} \langle n_b \rangle \\ = - \int_0^d dx D \frac{\partial}{\partial x} \langle n_b \rangle = 0, \end{aligned} \quad (67)$$

which completes the proof of Eq. (64). Equation (64) is significant in that the density-weighted average x location of the

electrons is conserved, however complicated the quasilinear evolution of the system. That is, combining Eqs. (63) and (64), we obtain

$$\bar{x} = \frac{\int_0^d dx x \langle n_b \rangle}{\int_0^d dx \langle n_b \rangle} = \text{const.} \quad (68)$$

(c) *Profile evolution*: We consider Eqs. (55) and (56) for $\gamma_k > 0$, and integrate Eq. (55) from $x=0$ to an arbitrary point x ($0 < x < d$). Enforcing the boundary condition $D=0$ at $x=0$ [Eq. (61)], we obtain

$$\frac{\partial}{\partial t} \int_0^x dx \langle n_b \rangle(x, t) = D \frac{\partial}{\partial x} \langle n_b \rangle, \quad (69)$$

or equivalently, from Eq. (59),

$$\frac{\partial}{\partial t} V_E(x, t) = D \frac{\partial^2}{\partial x^2} V_E. \quad (70)$$

Comparing with Fig. 3, it follows from Eqs. (69) and (70) that

$$\frac{\partial}{\partial t} \int_0^x dx \langle n_b \rangle \Big|_{t=0} \geq 0, \quad \text{for } x \leq x_m, \quad (71)$$

and

$$\frac{\partial}{\partial t} V_E \Big|_{t=0} \geq 0, \quad \text{for } x \leq x_m, \quad (72)$$

where $x = x_m$ corresponds to the density maximum in Fig. 3. That is, at a subsequent time $t_0 > 0$, the profiles for $\langle n_b \rangle$ and V_E have evolved to the form illustrated by the dashed curves in Fig. 3, corresponding to a weakening of the density gradients, and a partial fill-in of the density depression. Therefore, during the initial stages of instability, the quasilinear response of the system is in the direction of stabilization and reducing the growth rate [Eqs. (57) and (58)].

C. Resonant diocotron instability

As a specific example, we now consider the quasilinear evolution of the diocotron instability for the configuration illustrated in Fig. 4. This corresponds to a gentle density bump superimposed on the rectangular profile

$$\langle n_b \rangle = \begin{cases} \hat{n}_b = \text{const.}, & 0 < x < b, \\ 0, & b < x < d. \end{cases} \quad (73)$$

Such a configuration gives the weak resonant version^{4,5} of the diocotron instability discussed in Sec. III B, and the appropriate quasilinear equations describing the evolution of the system are given by Eqs. (55), (57), and (58), with diffusion coefficient D approximated by Eq. (62).

(a) *Real oscillation frequency*: For the configuration with gentle density bump illustrated in Fig. 4, the real frequency ω_k and eigenfunction $\delta \hat{\phi}_k(x)$ are calculated to good accuracy from the eigenvalue equation (58), approximating the density profile by the rectangular form in Eq. (73). The eigenvalue equation (58) becomes

$$\frac{\partial^2}{\partial x^2} \delta \hat{\phi}_k - k^2 \delta \hat{\phi}_k = \frac{k \delta \hat{\phi}_k \omega_d}{\omega_k - k V_E} \delta(x - b), \quad (74)$$

where $\omega_d = \hat{\omega}_{pb}^2 / \omega_c = 4\pi \hat{n}_b e c / B_0$, and the right-hand side of Eq. (74) corresponds to a surface-charge perturbation at $x = b$. Referring to Fig. 4, the solutions to Eq. (74) in region I

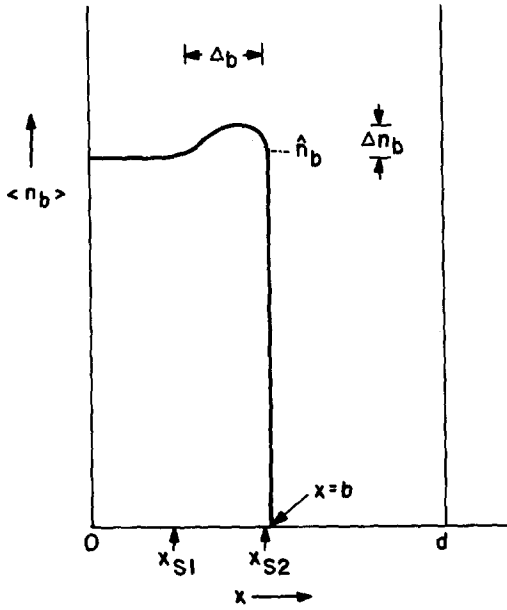


FIG. 4. Initial density profile $\langle n_b \rangle(x, 0)$ corresponding to weak resonant diocotron instability. The resonant region of x space satisfying $\omega_k - kV_E(x_s) = 0$ [Eq. (83)] covers the range $b^2/d \simeq x_{s1} < x_s < x_{s2} \simeq b$ [Eq. (86)].

($0 < x < b$) and region II ($b < x < d$) that are continuous at the surface ($x = b$) of the electron layer are

$$\delta\hat{\phi}_k^I = \hat{\phi}_k \sinh kx, \quad 0 < x < b, \quad (75)$$

$$\delta\hat{\phi}_k^{II} = \hat{\phi}_k \sinh kb \frac{\sinh k(d-x)}{\sinh k(d-b)}, \quad b < x < d,$$

where $\hat{\phi}_k$ is the amplitude (independent of x). Note from Eq. (75) that $\delta\hat{\phi}_k^I(x=0) = 0 = \delta\hat{\phi}_k^{II}(x=d)$ [Eq. (60)] at the cathode and anode. To determine ω_k , we integrate the eigenvalue equation across the surface at $x = b$ from $x_- = b(1 - \delta)$ to $x_+ = b(1 + \delta)$ and take the limit $\delta \rightarrow 0_+$. This gives

$$\left[\frac{\partial}{\partial x} \delta\hat{\phi}_k^{II} \right]_{x=b} - \left[\frac{\partial}{\partial x} \delta\hat{\phi}_k^I \right]_{x=b} = \frac{k [\delta\hat{\phi}_k^I]_{x=b} \omega_d}{\omega_k - kV_E(x=b)}. \quad (76)$$

Substituting Eq. (75) into Eq. (76) readily gives

$$\begin{aligned} & -\hat{\phi}_k \sinh kb \frac{\cosh k(d-b)}{\sinh k(d-b)} \\ & -\hat{\phi}_k \cosh kb = \frac{\omega_d \hat{\phi}_k \sinh kb}{\omega_k - kV_E(x=b)}. \end{aligned} \quad (77)$$

Solving Eq. (77) for the real oscillation frequency ω_k , we find

$$\omega_k - kV_E(x=b) = - \frac{\omega_d}{\coth kb + \coth k(d-b)}. \quad (78)$$

From Eqs. (59) and (73), it follows that $V_E(x=b)$ in Eq. (78) can be expressed as $V_E(x=b) = \omega_d b$, where $\omega_d = \hat{\omega}_{pb}^2 / \omega_c = 4\pi\hat{n}_b ec / B_0$.

In the short-wavelength limit, it follows from Eq. (78) that ω_k can be approximated by

$$\omega_k = kV_E(x=b)(1 - 1/2kb), \quad (79)$$

for $kb, k(d-b) \gg 1$. Moreover, for long wavelengths with $kb, k(d-b) \ll 1$, Eq. (78) gives

$$\omega_k = kV_E(x=b)(b/d). \quad (80)$$

A typical plot of ω_k vs kb is shown in Fig. 5 for $d/b = 2$.

(b) *Quasilinear growth rate*: Referring to Fig. 4, the resonant growth rate γ_k can be estimated from Eq. (51). Making use of $V_E = \omega_d x$ for $0 < x < b$ [Eq. (59)], and evaluating the $(\dots)^{-1}$ factor in Eq. (51) with $(\partial/\partial x)\langle n_b \rangle$ approximated by $-\hat{n}_b \delta(x-b)$, we obtain from Eq. (51)

$$\gamma_k = \pi \frac{[\omega_k - kV_E(b)]^2 |\delta\hat{\phi}_k^I|_{x=x_s}^2}{|kV_E(b)| |\delta\hat{\phi}_k^I|_{x=b}^2} \frac{b}{\hat{n}_b} \frac{\partial}{\partial x} \langle n_b \rangle \Big|_{x=x_s}. \quad (81)$$

In Eq. (81), $kV_E(b) = (kb)\omega_d$ and ω_k is determined from Eq. (78). Moreover, it follows from Eq. (75) that

$$\frac{|\delta\hat{\phi}_k^I|_{x=x_s}^2}{|\delta\hat{\phi}_k^I|_{x=b}^2} = \frac{\sinh^2 kx_s}{\sinh^2 kb}, \quad (82)$$

and the resonant location $x = x_s(k)$ is determined from $\omega_k - kV_E(x_s) = 0$ [Eq. (50)]. Note from Eq. (81) that $\gamma_k > 0$ (corresponding to instability) whenever x_s falls in the region of positive density slope in Fig. 4.

Combining Eq. (78) with $\omega_k - kV_E(x_s) = 0$ gives for $x_s(k)$,

$$k(b - x_s) = [\coth kb + \coth k(d-b)]^{-1}. \quad (83)$$

In the limits of short and long wavelengths, Eq. (83) reduces to the approximate results

$$x_s/b = (1 - 1/2kb), \quad \text{for } kb, k(d-b) \gg 1, \quad (84)$$

and

$$x_s/b = b/d, \quad \text{for } kb, k(d-b) \ll 1. \quad (85)$$

Therefore, from Eqs. (83)–(85), the resonant region of x space covers the range (see also Fig. 4)

$$b^2/d \simeq x_{s1} < x_s < x_{s2} \simeq b, \quad (86)$$

with the upper limit (x_{s2}) in Eq. (86) corresponding to short wavelengths, and the lower limit (x_{s1}) corresponding to long

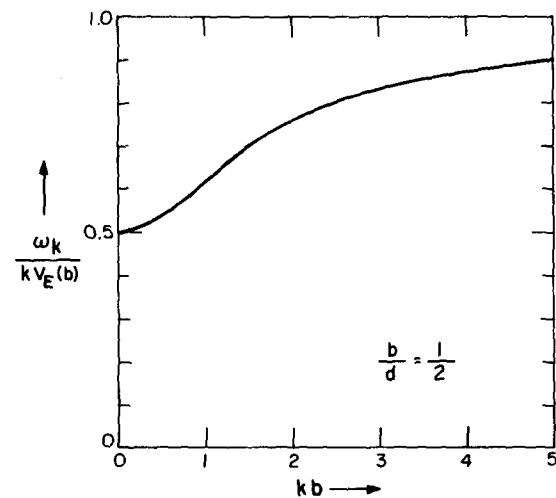


FIG. 5. Plot of normalized frequency $\omega_k/kV_E(b)$ vs kb obtained from Eq. (78) for $d/b = 2$.

wavelengths. Referring to Eq. (86) and Fig. 4, we find for $b/d = 1/2$ (for example) that x_s covers the range $1/2 \leq x_s/b \leq 1$.

Finally, it readily follows that the nonresonant region of x space satisfying $[\omega_k - kV_E(x)]^2 \gg \gamma_k^2$ corresponds to

$$\left(\frac{x - x_s}{b}\right)^2 \gg \frac{\gamma_k^2}{k^2 V_E^2(b)}, \quad (87)$$

where $V_E(b) = \omega_d b$, and γ_k and x_s are defined in Eqs. (81) and (83).

(c) *Quasilinear stabilization*: In the resonant region of x space satisfying $\omega_k - kV_E(x) = 0$, the quasilinear diffusion equation (55) for $\langle n_b \rangle$ can be expressed as

$$\frac{\partial}{\partial t} \langle n_b \rangle = \frac{\partial}{\partial x} \left(D_r \frac{\partial}{\partial x} \langle n_b \rangle \right), \quad (88)$$

where the resonant diffusion coefficient D_r is given by [Eq. (62)]

$$\begin{aligned} D_r &= \frac{16\pi^2 c^2}{B_0^2} \int_0^\infty dk \mathcal{E}_k \delta(\omega_k - kV_E) \\ &= \frac{16\pi^2 c^2}{B_0^2} \left[\frac{\mathcal{E}_k(x, t)}{|\partial \omega_k / \partial k - V_E|} \right]_{k=k_s(x)}. \end{aligned} \quad (89)$$

In Eq. (89), $k_s(x)$ solves the resonance condition $\omega_{k_s} - k_s V_E(x) = 0$, where $V_E(x) = \omega_d x$ and ω_k is defined in Eq. (78). Substituting Eq. (78) into $\omega_{k_s} = k_s V_E(x)$ gives the transcendental equation for $k_s(x)$:

$$k_s b [\coth k_s b + \cosh k_s(d - b)] = b/(b - x). \quad (90)$$

The spectral energy density \mathcal{E}_k in Eq. (89) of course evolves according to $(\partial/\partial t)\mathcal{E}_k = 2\gamma_k \mathcal{E}_k$ [Eq. (57)], where the linear growth rate $\gamma_k(t)$ is given in terms of $\langle n_b \rangle$ by Eq. (81).

An H theorem describing the stabilization process in the resonant region of x space ($x_{s1} \leq x \leq x_{s2}$) follows readily from Eqs. (88) and (89). Multiplying Eq. (88) by $\langle n_b \rangle$ and integrating over x gives

$$\begin{aligned} \frac{\partial}{\partial t} \int dx \langle n_b \rangle^2 &= - \int dx D_r \left(\frac{\partial}{\partial x} \langle n_b \rangle \right)^2 \\ &= - \frac{16\pi^2 c^2}{B_0^2} \int dx \int_0^\infty dk \delta(\omega_k - kV_E) \\ &\quad \times \mathcal{E}_k(x, t) \left(\frac{\partial}{\partial x} \langle n_b \rangle \right)^2 \leq 0. \end{aligned} \quad (91)$$

Analogous to the quasilinear stabilization of the one-dimensional bump-in-tail instability in velocity space,²⁰ the time-asymptotic ($t \rightarrow \infty$) solution inferred from Eq. (91) necessarily satisfies

$$\frac{\partial}{\partial x} \langle n_b \rangle(x, t \rightarrow \infty) \Big|_{x=x_s} = 0 \quad (92)$$

in the resonant region ($x_{s1} \leq x \leq x_{s2}$). We conclude from Eqs. (81) and (92) that

$$\gamma_k(t \rightarrow \infty) = 0, \quad (93)$$

corresponding to plateau formation and quasilinear stabilization of the instability. From Eq. (93) and $(\partial/\partial t)\mathcal{E}_k = 2\gamma_k \mathcal{E}_k$, we conclude that the spectral energy density saturates at a steady asymptotic level $\mathcal{E}_k(x, \infty)$.

(d) *Estimate of saturation level*: To obtain a detailed estimate of the saturation level of the instability, it is generally

necessary to solve the coupled quasilinear kinetic equations for $\langle n_b \rangle$ and \mathcal{E}_k for specified initial profile $\langle n_b \rangle(x, 0)$. To obtain a simple order-of-magnitude estimate, however, it is adequate to make use of the conservation relation satisfied by $\int dx x \langle n_b \rangle$ in the resonant region. Multiplying $(\partial/\partial t)\langle n_b \rangle = (\partial/\partial x)(D_r \partial \langle n_b \rangle / \partial x)$ by x and integrating over x for the resonant particles gives

$$\begin{aligned} \left(\frac{\partial}{\partial t} \int dx x \langle n_b \rangle \right)_r &= - \frac{8\pi^2 c^2}{B_0^2} \int dx \int dk \mathcal{E}_k \delta(\omega_k - kV_E) \frac{\partial}{\partial x} \langle n_b \rangle \\ &= - \frac{8\pi^2 c^2}{B_0^2} \int dk \frac{\mathcal{E}_k(x_s, t)}{|kV_E(b)|} b \frac{\partial}{\partial x} \langle n_b \rangle \Big|_{x_s}, \end{aligned} \quad (94)$$

where $x_s(k)$ solves $\omega_k - kV_E(x_s) = 0$ [Eq. (83)], and use has been made of $V_E(x) = \omega_d x$ and the definition of D_r in Eq. (62). Making use of Eq. (81) to eliminate $(\partial/\partial x)\langle n_b \rangle|_{x=x_s}$, we can express Eq. (94) as

$$\begin{aligned} \left(\frac{\partial}{\partial t} \int dx x \langle n_b \rangle \right)_r &= - \frac{4\pi c^2 \hat{n}_b}{B_0^2} \int dk \frac{2\gamma_k \mathcal{E}_k(b, t)}{[\omega_k - kV_E(b)]^2} \\ &= - \frac{4\pi c^2 \hat{n}_b}{B_0^2} \frac{\partial}{\partial t} \int dk \frac{\mathcal{E}_k(b, t)}{[\omega_k - kV_E(b)]^2}, \end{aligned} \quad (95)$$

where use has been made of $(\partial/\partial t)\mathcal{E}_k = 2\gamma_k \mathcal{E}_k$ and $\mathcal{E}_k(x_s, t) = \mathcal{E}_k(b, t) |\delta \hat{\phi}_k|_{x=x_s}^2 / |\delta \hat{\phi}_k|_{x=b}^2$, and the time variation of ω_k has been neglected in Eq. (95). Integrating Eq. (95) with respect to time gives the conservation relation

$$\begin{aligned} \Delta \left(\int dx x \langle n_b \rangle \right)_r &= - \frac{4\pi c^2 \hat{n}_b}{B_0^2} \Delta \left(\int dk \frac{\mathcal{E}_k(b, t)}{[\omega_k - kV_E(b)]^2} \right), \end{aligned} \quad (96)$$

where ΔF denotes $F(t) - F(t=0)$. As a point of consistency, if we make use of Eq. (62) for D_r and the approximate form of $\langle n_b \rangle$ given in Eq. (73) in evaluating $\int dx D_r (\partial/\partial x)\langle n_b \rangle$ for the nonresonant particles, then it is straightforward to show

$$\left(\frac{\partial}{\partial t} \int dx x \langle n_b \rangle \right)_r + \left(\frac{\partial}{\partial t} \int dx x \langle n_b \rangle \right)_{nr} = 0, \quad (97)$$

which is consistent with the conservation law (64) proved in Sec. IV B in the general case.

Equation (96) can be used to estimate the $t \rightarrow \infty$ saturation level of the perturbed fields. For present purposes, we make use of Eq. (78) to estimate $[\omega_k - kV_E(b)]^{-2} \approx 1/\omega_d^2$ in the integrand in Eq. (96), and denote the change in perturbed field energy density by $\Delta \mathcal{E}_F(t) = \int dk \mathcal{E}_k(b, t) - \int dk \mathcal{E}_k(b, 0)$. Equation (96) then gives the order-of-magnitude estimate

$$\Delta \left(\int dx x \langle n_b \rangle \right)_r \approx - \frac{4\pi c^2 \hat{n}_b}{B_0^2 \omega_d^2} \Delta \mathcal{E}_F. \quad (98)$$

As a simple model to estimate the left-hand side of Eq. (98), we assume that $\langle n_b \rangle$ initially has the linear profile $\hat{n}_b + (\Delta n_b / \Delta_b)[x - (b - \Delta_b/2)]$ over the interval $b - \Delta_b < x < b$ at $t = 0$, and the flat profile \hat{n}_b as $t \rightarrow \infty$. That is, the initial density gradient in the bump region is assumed

to be $(\partial/\partial x)\langle n_b \rangle = \Delta n_b/\Delta_b$, where Δ_b is the width of the density bump. Equation (98) then gives

$$\begin{aligned}\Delta \mathcal{E}_F(\infty) &\approx \frac{1}{6} \frac{\Delta n_b}{\hat{n}_b} \frac{\Delta_b^2 \omega_d^2}{c^2} \frac{B_0^2}{8\pi} \\ &= \frac{1}{6} \frac{\Delta n_b}{\hat{n}_b} \frac{\Delta_b^2}{b^2} \frac{V_E^2(b)}{c^2} \frac{B_0^2}{8\pi} \\ &= \frac{1}{6} \frac{\Delta n_b}{\hat{n}_b} \frac{\Delta_b^2}{b^2} \frac{\langle E_x(b) \rangle^2}{8\pi}.\end{aligned}\quad (99)$$

Here, $\omega_d = \hat{\omega}_{pb}^2/\omega_c = 4\pi\hat{n}_b ec/B_0$, $V_E(b) = \omega_d b$, and $\langle E_x(b) \rangle = -4\pi e\hat{n}_b b$ for the configuration considered here.

Equation (99) gives a useful order-of-magnitude estimate for the saturation level of the perturbed field for an initially unstable configuration characterized by a small density bump (Δn_b) with spatial width Δ_b . Assuming that the saturated field level ($t \rightarrow \infty$) is much larger than the initial field level, then $\Delta \mathcal{E}_F(\infty) \simeq \int dk \mathcal{E}_k(b, \infty)$. Moreover $\int dk \mathcal{E}_k(b, \infty) = \int dk k^2 |\delta\phi_k(b, \infty)|^2/8\pi = \langle \delta E_y^2(b, \infty) \rangle/8\pi$. Therefore, Eq. (99) reduces to

$$\langle \delta E_y^2(b, \infty) \rangle \approx \frac{1}{6} \frac{\Delta_b^2}{b^2} \frac{\Delta n_b}{\hat{n}_b} \langle E_x(b) \rangle^2. \quad (100)$$

It is clear from Eq. (100) that the perturbed fields can saturate at a substantial level, even for a moderately small density bump as measured by $\Delta n_b/\hat{n}_b$.

V. CONCLUSIONS

In the present analysis, a macroscopic cold-fluid model was used to investigate the quasilinear stabilization of the diocotron instability for sheared, nonrelativistic electron flow in a planar diode (Fig. 1). The nonneutral electron plasma was treated as a massless ($m \rightarrow 0$) guiding-center fluid with flow velocity $\mathbf{V}_b = -(c/B_0)\nabla\phi \times \hat{\mathbf{e}}_z$ (Sec. II), and the continuity-Poisson equations were used to obtain coupled quasilinear kinetic equations describing the self-consistent evolution of the average density $\langle n_b \rangle(x, t)$ and spectral energy density $\mathcal{E}_k(x, t)$ associated with the y electric field perturbations (Sec. III). Several general features of the quasilinear evolution of the system were discussed in Sec. IV including a derivation of exact conservation constraints. Typically, if the initial profile $\langle n_b \rangle(x, t=0)$ corresponds to instability with $\gamma_k(0) > 0$, the perturbations amplify [Eq. (57)], and the density profile $\langle n_b \rangle(x, t)$ readjusts [Eq. (55)] in such a way as

to reduce the growth rate $\gamma_k(t)$ and stabilize the instability [Eqs. (57) and (58)].

Finally, as a specific example, in Sec. IV C we considered the quasilinear evolution of the diocotron instability for $\langle n_b \rangle(x, 0)$ corresponding to a gentle density bump superimposed on a rectangular density profile in contact with the cathode (Fig. 4). Such a configuration gives a weak version of the diocotron instability. It was shown that the system stabilizes time asymptotically by plateau formation [Eqs. (92) and (93)] in the resonant region of x space where $\omega_k - kV_E(x) = 0$. Making use of the quasilinear equations to obtain an order-of-magnitude estimate [Eq. (100)] of the saturation level of the perturbed fields, it was shown that $\langle \delta E_y^2(b, \infty) \rangle/8\pi \approx (1/6)(\Delta_b/b)^2(\Delta n_b/\hat{n}_b)\langle E_x(b) \rangle^2/8\pi$, where Δn_b and Δ_b are the characteristic height and width, respectively, of the density bump (Fig. 4).

ACKNOWLEDGMENTS

This research was supported by Sandia National Laboratories and in part by the Office of Naval Research.

- ¹G. C. MacFarlane and H. G. Hay, Proc. R. Soc. London Ser. B **63**, 409 (1950).
- ²R. H. Levy, Phys. Fluids **8**, 1288 (1965).
- ³O. Buneman, R. H. Levy, and L. M. Linson, J. Appl. Phys. **37**, 3203 (1966).
- ⁴R. J. Briggs, J. D. Daugherty, and R. H. Levy, Phys. Fluids **13**, 421 (1970).
- ⁵R. C. Davidson, *Theory of Nonneutral Plasmas* (Benjamin, Reading, MA, 1974), pp. 66–78, and references therein.
- ⁶R. C. Davidson and K. Tsang, Phys. Rev. A **29**, 488 (1984).
- ⁷D. Chernin and Y. Y. Lau, Phys. Fluids **27**, 2319 (1984).
- ⁸Y. Y. Lau, Phys. Rev. Lett. **53**, 395 (1984).
- ⁹R. L. Kyhl and H. F. Webster, IRE Trans. Electron Devices **3**, 172 (1956).
- ¹⁰C. A. Kapetanakis, D. A. Hammer, C. D. Striffler, and R. C. Davidson, Phys. Rev. Lett. **30**, 1303 (1973).
- ¹¹K. R. Prestwich, D. E. Hasti, R. B. Miller, and A. W. Sharpe, IEEE Trans. Nucl. Sci. NS-30, 3155 (1983).
- ¹²G. Rosenthal, G. Dimonte, and A. Wong (private communication).
- ¹³O. Buneman, *Crossed-Field Microwave Devices* (Academic, New York, 1961).
- ¹⁴S. Y. Liao, *Microwave Devices and Circuits* (Prentice-Hall, Englewood Cliffs, NJ, 1980).
- ¹⁵R. C. Davidson, K. Tsang, and J. Swegle, Phys. Fluids **27**, 2332 (1984).
- ¹⁶J. Swegle, Phys. Fluids **26**, 1670 (1983).
- ¹⁷J. Swegle and E. Ott, Phys. Fluids **24**, 1821 (1981); J. Swegle and E. Ott, Phys. Rev. Lett. **46**, 929 (1981).
- ¹⁸J. P. Van Devender, J. P. Quintenz, R. J. Leeper, D. J. Johnson, and J. T. Crow, J. Appl. Phys. **52**, 4 (1981).
- ¹⁹R. C. Davidson, in *Handbook of Plasma Physics*, edited by M. N. Rosenbluth and R. Z. Sagdeev (Elsevier Science, New York, 1984), Vol. 2, pp. 731–819.
- ²⁰R. C. Davidson, *Methods in Nonlinear Plasma Theory* (Academic, New York, 1972), pp. 174–182.